3 Measures of forest fragmentation at varying spatial resolutions, a study from central Italy

The purpose of the analysis carried out in this chapter was to investigate the potential of using spatial metrics to describe the structure of a forested landscape, and to investigate further how these metrics behave when calculated at different scales and based on different input data types. The analyses carried out here formed part of studies for the Eurolandscape project, where selection of indices for forest structural assessment at the European level was one of the work packages. The early phases of that work concentrated on some relatively simple measures, which also had the advantage of being possible to control visually by comparison with the input data, in this case images classified into forest-non/forest maps.

One commonly used approach for examination of scaling (grain size) effects is to spatially degrade raster data (high resolution imagery) that is assumed to express the "real" situation, i.e. the "true" shape and distribution of forest patches (Turner *et al* 1989). Here, it was investigated whether the use of spatial indices can assist in the scaling process or deliver supplemental information about it. A particularly important task, given the data available and considerations of data costs, was to investigate the possibility of relating the values of spatial indices derived from medium resolution data (e.g. WiFS-based forest maps) to those derived from high-resolution data or detailed forest/land cover maps. If such relations were established, it could make possible the extraction of information at the scale where processes important to ecosystems take place. A part of the justification for this study was to look deeper into the usefulness of the two new metrics proposed by Frohn (1998) and to compare them with the better known and more commonly used Matheron index.

3.1 Methodology

The first step included simulation of how a forested landscape appears as raster images from EO sources at different spatial resolutions (pixel or grain sizes). The indices mentioned in

section 2.3.4 were calculated for the same cells or sub-landscape, thus assessing the influence of the apparent aggregation and isolation processes which are known to take place when changing sensor or pixel size (Bian 1997, Cao and Lam 1997). The forest-non-forest maps with different resolutions were derived from a synthetic image, produced by assigning pixel values to the cells of a grid, from a vector coverage. The initial (base) image was the one with the highest spatial resolution, i.e. smallest pixel size; this cell size can be as small as the resolution of the data from which the maps or GIS coverages were originally made. Images at coarser resolution were made by majority filtering of the binary images, using gradually larger kernels (2, 4, 8 and finally 16 pixels).

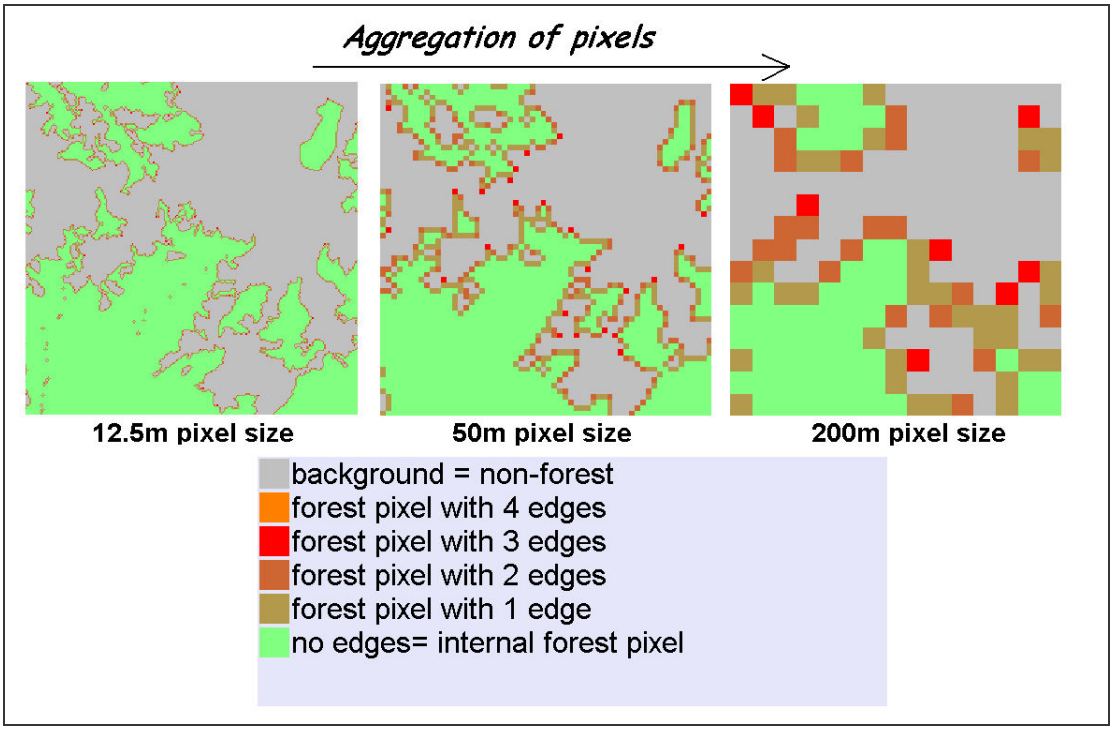

Figure 3.1 Aggregation of pixels from synthetic forest-non-forest image A 3*3 km subset is shown here, similar to one of the windows used for calculation of spatial metrics.

In the second step, real satellite images were used and the effort focused on establishing relations between the spatial measures derived from forest/non-forest images for cells or sub-landscapes of the same spatial extent but necessarily of different size measured in pixels. Even when this was not possible, the results point to some reasons why scaling or multi-sensor problems occur.

Assuming that a linear relation exists between spatial scale, expressed as grain size (in this case equal to pixel size) and the values of the metrics, a relation like this is expected:

$$SM = Ap+B$$

Where SM is the actual spatial metric, p is the pixel size (diameter or edge length), A and B are coefficients characteristic to the dataset or data type in question, such as the geographic region or the type of land cover map. This follows the methods of Benson and MacKenzie (1995) and Turner *et al* (1989), although in the latter study, the regressions were performed between metric values and the log of the aggregate pixel size.

The task of generating forest maps from remotely sensed data is not a trivial one (McGwire 1992, Häusler *et al* 1993, Mayaux and Lambin 1995 and 1997), so for this study a robust and proven approach had to be selected. Because emphasis was on correct description of spatial structure rather than classification accuracy, it was decided to do unsupervised classification of the satellite images from the study area, in order apply the same approach to the two types of satellite data used here. For each of the multi-spectral images, a number of spectral clusters are identified and each pixel in the image assigned to the nearest one. After inspection of Red-Near Infrared 'scattergrams' (see Figure 3.13 and Figure 3.14), of CLC data and of the GIS data (a regional, administrative forest map), the spectral classes were assigned to either forest or non-forest.

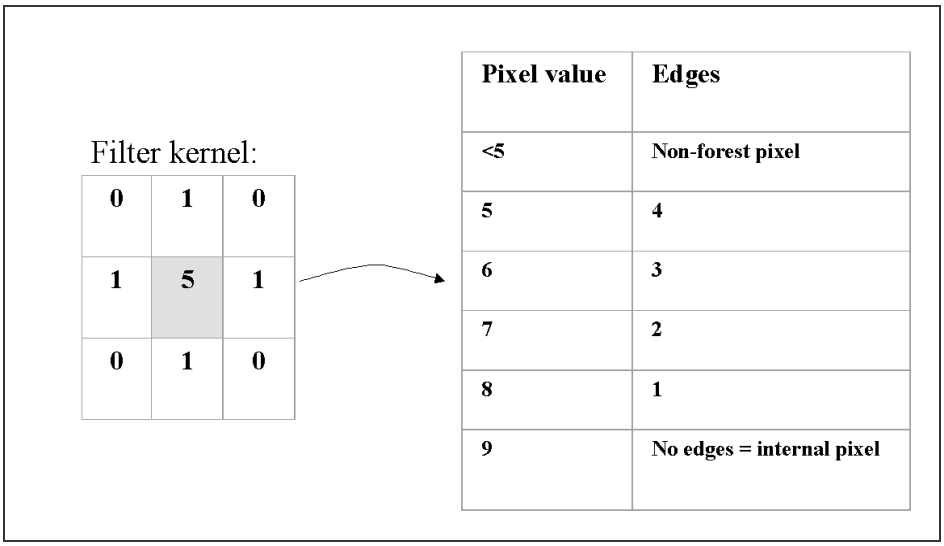

Figure 3.2 Extraction of edge (count) data from binary (forest-non-forest) images.

The map images were then filtered at each resolution, as illustrated in Figure 3.2. This was done for two reason, first to provide input to edge-counting for calculation of the Matheron and the SqP indices and secondly for illustrations of the effects of spatial degradation, as they e.g. appear in Figure 3.1.

Assuming that the satellite images, the results of the classifications, and the land cover maps made from these describe a landscape, it follows that in order to meaningfully apply metrics that describe the structural variation within the landscape which is important for its stability (Kareiva and Wennergren 1995), smaller subsets of these maps (sub-landscapes) must be used. For that reason it was found appropriate to use a modified version of the Fragstats software package (McGarigal and Marks 1994), in order to make it possible to apply a "moving-window" approach. This approach was developed and applied in a study carried out for the FIRS project (Häusler *et al* 2000), as part of a study financed by the Directorate General VI of the European Commission, called "Pilot Study in the Field of Monitoring Forested Areas"[9]. The aim of the project was to demonstrate satellite based methods for the operational assessment of changes and structural diversity of European Forest Ecosystems and

[9] (Contract N° 9662CO001), carried out by a European Consortium lead by GAF, Munich. The name of DG VI has since been changed to DG Agriculture.

to define the requirements for the implementation of a monitoring system, and the use of spatial indices was considered a natural part of such a system. The outputs from the calculation of the various metrics are initially stored in table format in text-files (or files that can be read using any text editing software tool). These files can be imported into spreadsheets for statistical analysis, or converted to three-dimensional grids using e.g. Surfer (Keckler 1997), or even directly imported (as ASCII files, given the number of rows and columns is known) into image processing programs. Back in an image processing environment the grids can be edited, typically by adding header-information to, once again be geo-referenced, and thus used in combination with GIS data vector layers or other raster images.

The image processing software used for this study was WinChips (Hansen 2001), statistical processing and drawing of graphs was done with the Microsoft Excel spreadsheet. Calculation of the Matheron index is not implemented in Fragstats, thus this index was calculated from image statistics extracted for each grid cell of an (Arc-View format) shape-file, using the grids shown in Figure 3.5 and Figure 3.6. In this particular case the method applied was calculation of spatial metrics in moving windows *without overlap*, thus there are no smoothing effects.

3.2 Data

The test site is an intensively forested area, located in the Italian region of Umbria near the city of Foligno (south of Perugia), in the Apennine Mountains. The forests are mainly deciduous in composition, and are made up of oak, beech, and other species. The forests are managed using both coppice and high-forest silvicultural systems. The topography is mountainous, with elevation from 207 to 1425 metres above sea level. The test site is located in Landsat TM scene 191-030, with the scene centre at 43.30 latitude, 12.75 longitude.

The Landsat TM data were acquired as part of a study on the application of the Forest Light Interaction Model (FLIM) for mapping forest structural parameters, following the approach

described by McCormick (1996). A sub scene of an image acquired 12th July 1996 was extracted, 50*50 kilometres in extent. This image was ortho-rectified to UTM projection using a digital terrain model. Only bands 3, 4, and 5 have been used. An area of slightly greater extent than the subscene was described in detail by a GIS coverage of forest types and properties (Grohmann 2000), made at the forest department of the Regione di Umbria. The nominal resolution of Landsat TM images is 28.5*28.5m, in this study the images were rectified to pixel size 25*25 m.

	Landsat TM		IRS WiFS	
	band nr.	wavelgt. µm	band nr.	wavelgt. µm
Red	3	0.63-0.69	1	0.62-0.68
NIR	4	0.76-0.90	2	0.77-0.86
MIR	5	1.55-1.75		

Table 3.1 Satellite data used for forest mapping.

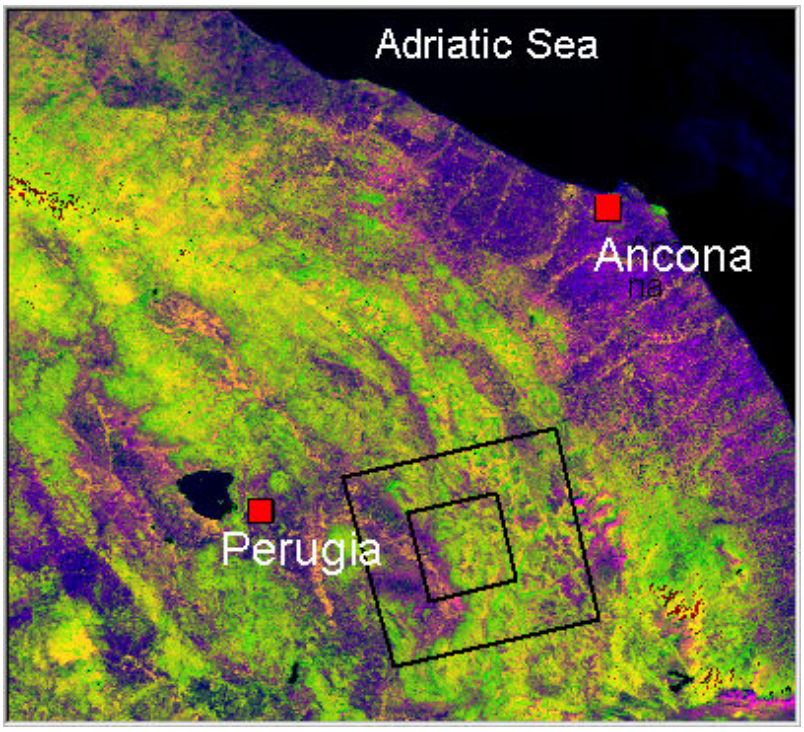

Figure 3.3 Location of the test areas, shown on false colour WiFS image, red band = WiFS channel 2 (NIR), green band = NDVI ((b2-b1)/(b2+b1)), blue band = WiFS channel 1 (red refl.). Forested areas are seen as green/yellow, agricutural areas as red/blue. The image was acquired 2. Sept. 1997, the extent is the same as a full Landsat scene, i.e. 180*180 km.

The WiFS data were acquired on Sep. 2 1997, and has been used in a pilot study about forest mapping at regional scales by medium resolution data, carried out at VTT, Finland (Häme *et al* 1999). The data have undergone atmospheric correction using the 6S code (Tanre *et al* 1992) and a BiDirectional Reflectivity Function (BDRF) correction for surface topography. The data were supplied in the projection of the CORINE land cover database (Lambert Azimutal) re-projected to Universal Transverse Mercator (UTM) zone 33 coordinates, and finally had to be shifted to fit the TM data exactly, by interactive inspection and changing offset values of the two images. The locations of the subsets used in this study, the 50*50 km TM and WiFS images and the 25*25 km synthetic image are shown in Figure 3.3. The nominal resolution of the WiFS sensor is 180 m, the data used here were rectified to a pixel size of 200 m. The spectral characteristics of the satellite data used are shown in Table 3.1.

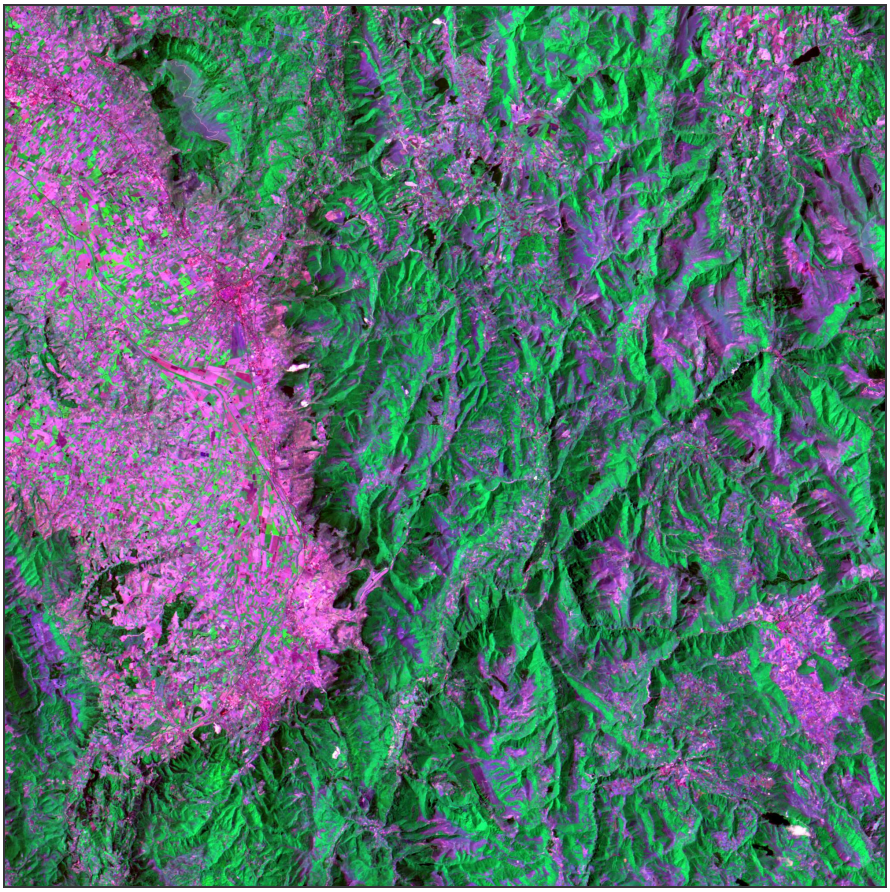

Figure 3.4 Geo-rectified subset of the Landsat TM scene recorded 12 July 1996, bands 3 (red), 4(green) and 5 (blue), extent 50 km. Agricultural fields, dominant in the Val Umbra to the left (west) appear red, grasslands bright green and forest in darker green shades.

3.3 Results

In this section, the main findings from simple statistical analysis of the results from image processing and calculation of spatial metrics are presented, with focus on scaling effects. Also the display of the calculated spatial metrics and in map-form and graphical display of their scaling behaviour are addressed.

3.3.1 Synthetic images, scaling properties

All forest class layers of the GIS coverage were combined and used for creating a raster image that could simulate high resolution satellite imagery. The pixel size was set to 12.5m, and the extent of this image was 25*25km. The image was then gradually degraded to pixel sizes of 25, 50, 100 and 200 m, as described in the previous section. For each image SqP, PPU and M were calculated for each cell, in this case the image was viewed as 64 cells of each 3*3 km, thus excluding the the southernmost and easternmost edge areas, as seen in Figure 3.5 and Figure 3.6. These figures also show the two extremes in form of the initially created image and the result of the last degradation step.

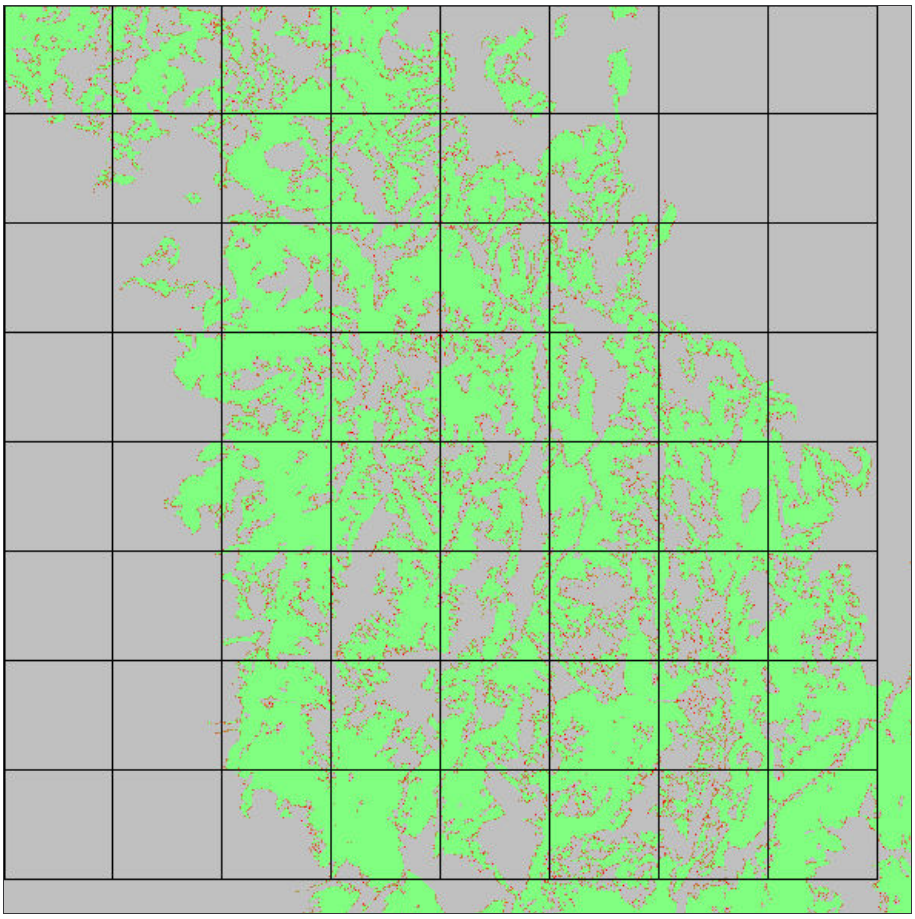

Figure 3.5 Synthesised forest mask, pixel size 12.5 m., after edge detection. Forest appear as green, background as grey, edge pixels in red and brown, same legend as in Figure 3.1. Image extent 25*25 km, grid cell size 3*3 km.

Windows with no forest cover were excluded from the calculations of M and SqP, since these indices are undefined when the number of forest pixels is zero. For all metrics and at each resolution the results were plotted against the forest area. The most striking observation here was the non-linear relation between the number of patches (per unit) and the total forest area (calculated for the start-image with 12.5m resolution) within the grid cell, as illustrated in Figure 3.7.

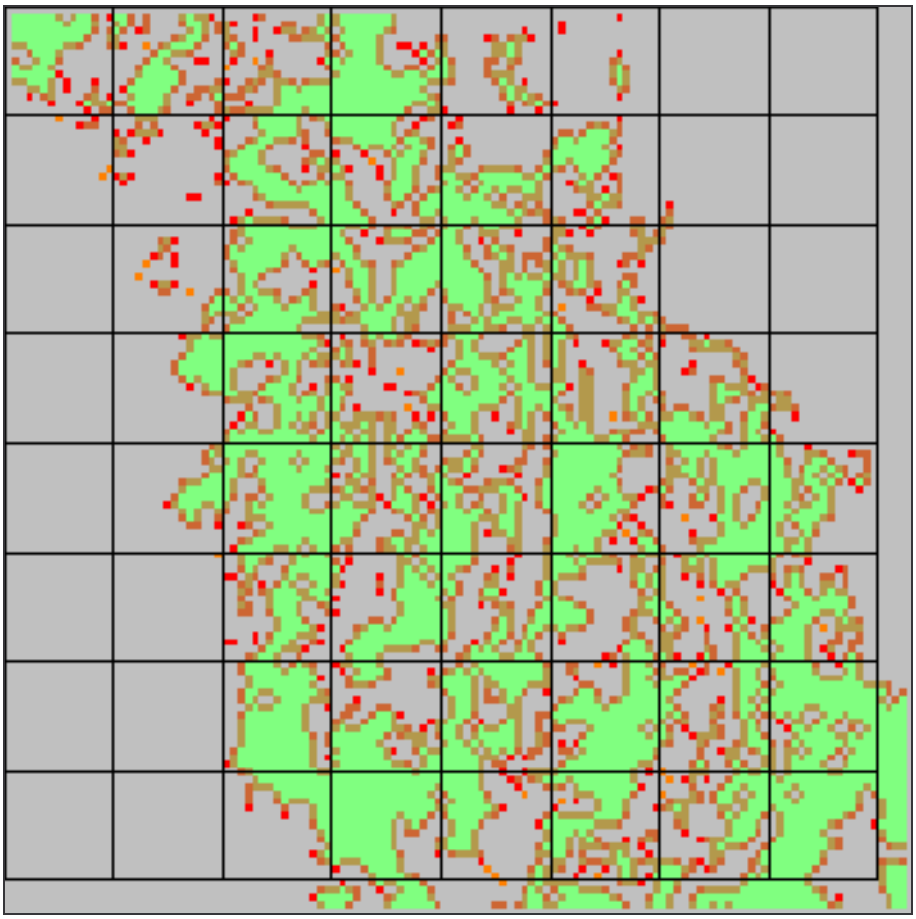

Figure 3.6 Synthesised forest mask, pixel size 200 m, after edge detection. Colouring as for Figure 3.1.

After the initial inspection of the results, it also appeared that especially the SqP values were related to the forest area. The indices are seen either to increase or decrease uniformly with the coarsening of the image, but a dependence on the type of the input cells was found with regard to forest cover percentage and to the number of patches. Regressions performed on the averaged values of the three metrics and the resolution as expressed by pixel size (p) gave the following results:

$$\mathbf{SqP = 0.8359 - 0.0013p,\ R^2 = 0.99}$$

$$\mathbf{PPU = 1.66 - 0.00083p,\ R^2 = 0.64}$$

$$\mathbf{M = 1.33 + 0.0222p,\ R^2 = 0.93}$$

These scaling relations are characteristic of this particular landscape, or landscape type, and can in principle be used for the prediction of metrics values at finer spatial resolutions from values calculated at coarser ones.

3.3.2 Synthetic images, metrics behaviour

For this part of the analysis, the values of the spatial metrics were grouped according to the percentage of the area that is forested, in order to further investigate the behaviour of the metrics with changing resolution, and to confirm or reject the assumption the they behave differently with different forest cover proportions. The groups were selected based on visual inspection of plots such as shown in Figure 3.7 and Figure 3.8, in such a way that they would contain the same number of samples.

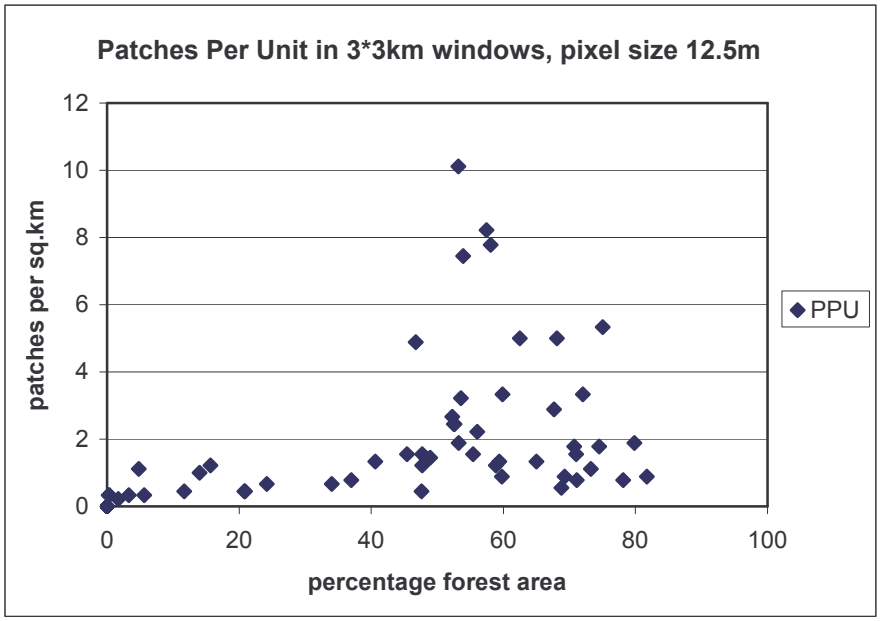

Figure 3.7 Patch density in synthetic forest map plotted against forest cover in each window. The number of patches per unit peaks when about half of the grid cell is forest covered.

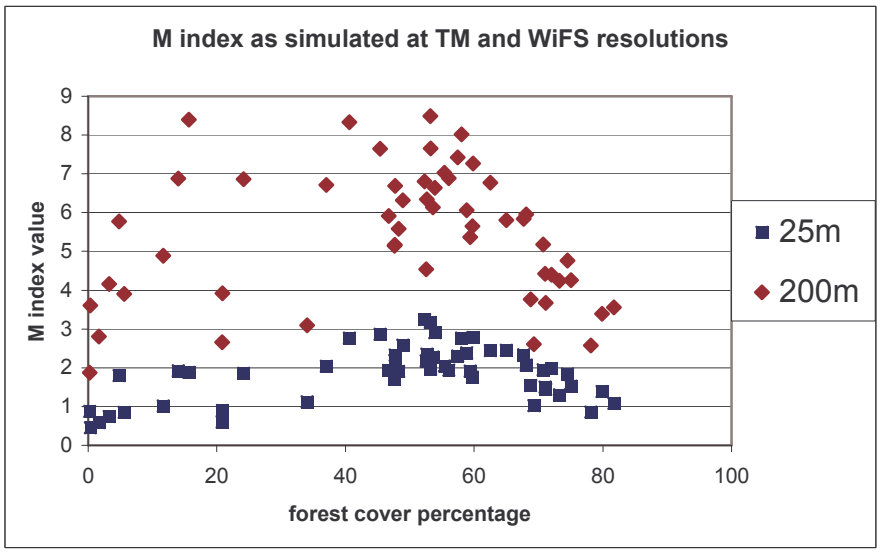

Figure 3.8 Pixel size influence on Matheron index values, shown by per-window plots of M values against forest cover for 25 and 200m grain sizes respectively.

From Figure 3.9 and Figure 3.10, it appears that both the SqP and the PPU metrics have their highest values when about half of the landscape is covered by forest. The decline in SqP with increasing pixel size is due to the relatively larger amount of interior or non-edge pixels in images at high spatial resolution, see also Figure 3.1. The fact that the values of SqP become smaller with increasing pixel size, is in accordance with the less complex shapes observed at lower resolutions, due to the "filtering out" of small patches with a high edge/area ratio, narrow linear patches and "gaps" within forest patches. The SqP values are surprisingly predictable under spatial degradation, thus the best metric for multi-scale comparisons, even between 12.5m and 200m pixel size.

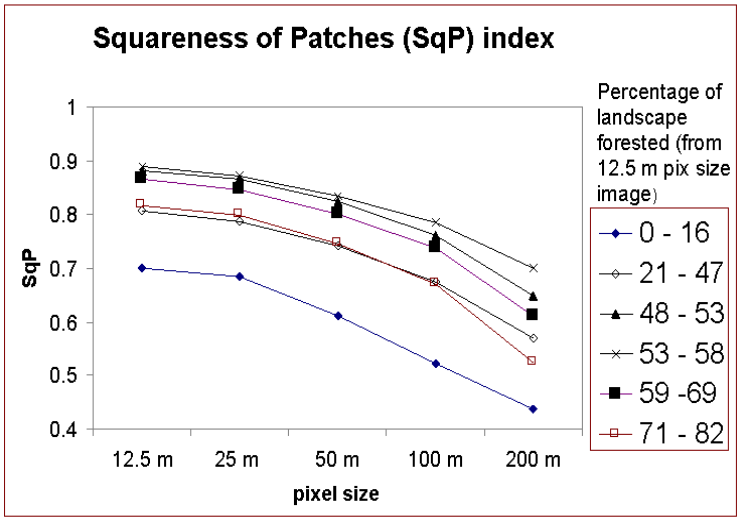

Figure 3.9 SqP as function of pixel size and forest cover for synthetic images. The values are grouped by amount of forest cover in the windows for which they were calculated.

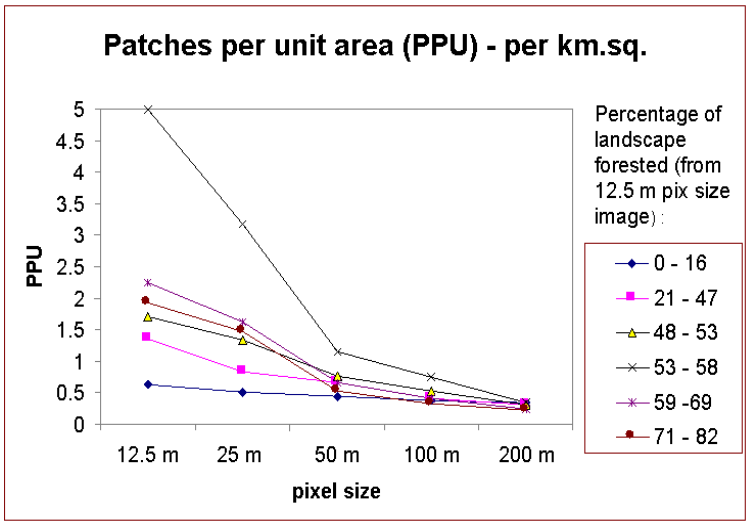

Figure 3.10 PPU as function of pixel size and forest cover (grouping as above) for synthetic images. Most patches are "lost" during the initial phase of pixel size degradation.

The decline of the PPU values is strongest in the initial phase of degradation, probably due to the effect of eliminating patches consisting of one or a few pixels. The values of the metrics within each window at each resolution were regressed, along with the amount of forest cover in the cell, and the correlation coefficients are shown in Table 3.2 and Table 3.3. The results indicate that SqP is a more robust metric for comparison across scales.

SqP	*Area12.5*	*12.5*	*25*	*50*	*100*
Area12.5	1				
12.5	0.533924	1			
25	0.526287	0.997263	1		
50	0.50381	0.990373	0.991971	1	
100	0.472774	0.970723	0.974048	0.987853	1
200	0.343242	0.918761	0.928397	0.936453	0.96009

Table 3.2 Correlation of the SqP metric derived from different pixel sizes. n=53

PPU	*Area12.5*	*12.5*	*25*	*50*	*100*
Area12.5	1				
12.5	0.480305	1			
25	0.498294	0.912379	1		
50	0.460977	0.726954	0.805893	1	
100	0.42592	0.589735	0.690656	0.877039	1
200	0.350249	0.372709	0.358311	0.668289	0.764104

Table 3.3 Correlation of the PPU metric derived from different pixel sizes. n=64

The Matheron index, M was found to increase with increasing pixel size, again a consequence of the higher perimeter to area ratio. The response curves in Figure 3.11 show that M assumes its highest values when around half of the window is covered by forest, while no relation is observed between the number of patches and the ordering of the curves in Figure 3.12. These findings contrast with the better correlation between M and NP (equivalent to PPU) than between M and the forested area, as presented in Table 3.4. This is possibly due to the limited number of samples used in this study, where extreme values in one window can seriously affect the average value for the (patch number or coverage) interval.

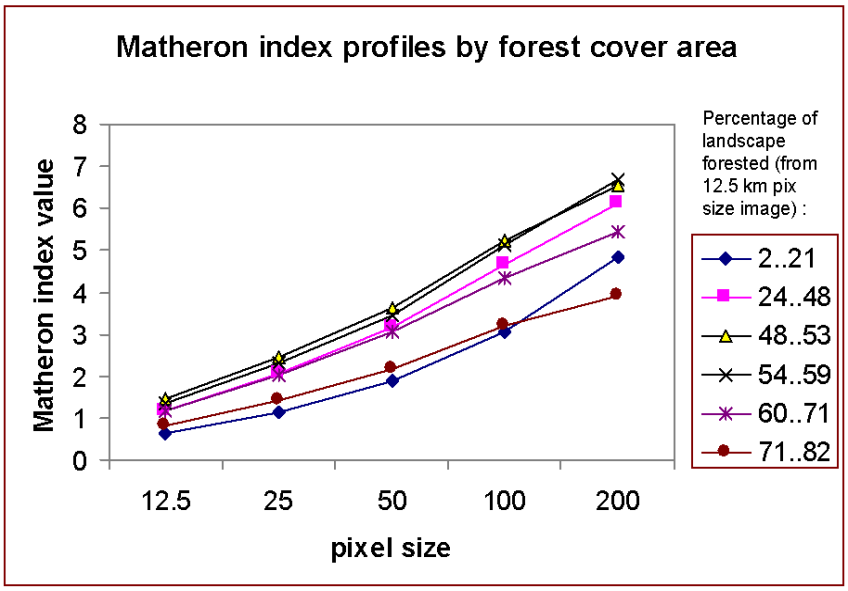

Figure 3.11. M values as function of pixel size and forest cover for synthetic images. The results were grouped according to percentage of landscape forested in the window.

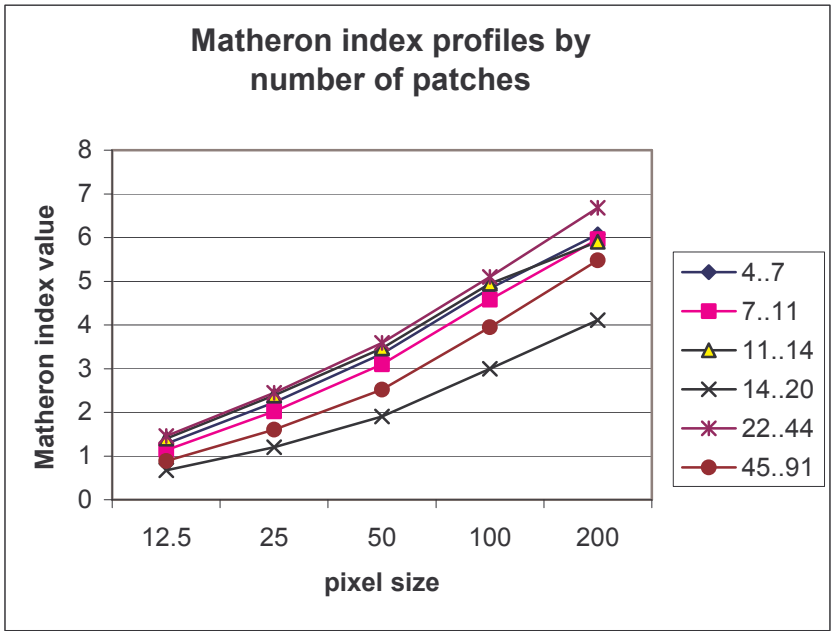

Figure 3.12. M values as function of pixel size and number of patches for synthetic image. The results were grouped according to the number of forest patches in the window (a number proportional to PPU).

Regression between the M values in each of the 53 windows with forest present (Table 3.4) shows this measure to be stable with changing resolution, though not as well as the SqP index. The findings of this part of the study indicate that it is possible to compare at least some landscape structure measures derived from images of different resolution, assuming that the behaviour of the sensors are simulated correctly by the spatial degradation.

Matheron	*Area (12.5m)*	*NP*	*12.5*	*25*	*50*	*100*
Area (12.5m)	1					
NP	0.33494	1				
M(12.5m)	0.371358	0.623638	1			
M(25m)	0.367724	0.585393	0.993583	1		
M(50m)	0.324514	0.559507	0.978305	0.990239	1	
M(100m)	0.287044	0.519934	0.930624	0.951433	0.965819	1
M(200m)	0.066402	0.491389	0.809905	0.83091	0.858397	0.923352

Table 3.4 Correlation between M derived at varying pixel sizes, forest cover as derived from the 12.5 m pixel size image and number of patches within each window. N=53.

Finally, it was found that the values of the spatial metrics correlate to each other in similar ways at 'coarse' as at 'fine' resolutions when degraded, as shown in Table 3.5, while the values get 'decoupled' from their relation to (initial) forest area. The M and the SqP metrics are more correlated with each other than with the PPU metric, which is not surprising since they both depend on edge-counts and area measures, while PPU values only depend on patch counts.

25m grain	*Area12.5*	*SqP25*	*PPU25*		*200m grain*	*Area12.5*	*SqP200*	*PPU200*
Area12.5	1				Area12.5	1		
SqP25	0.560686	1			SqP200	0.33633	1	
PPU25	0.343091	0.48181	1		PPU200	-0.1605	0.465624	1
M25	0.367724	0.888674	0.610049		M200	-0.03194	0.818425	0.555968

Table 3.5 Correlations between initial forest area and the three spatial metrics from synthetic images at resolutions corresponding to imagery from the TM and WiFS sensors.

3.3.3 Satellite images, classification and mapping

It was attempted to classify the TM and the WiFS data with methods as similar as possible, and the unsupervised classification yielding 40 classes was performed for each image. As illustrated in Figure 3.13 and Figure 3.14, 19 of the spectral classes from the WiFS image and also 19 out of 40 classes from the TM image were chosen to make up the forest masks, that ware used in the further analysis. The three 'possible forest classes' indicated in Figure 3.13 were mostly found in the western part of the scene, which is dominated by agriculture, and

may be olive groves or other plantations mistaken for forest. It was chosen to keep these classes as forest in order to avoid fragmentation effects in the areas that was known to be forest according to the GIS coverage, although the classification result obviously looked more perforated than the synthesised coverage (e.g. compare Figure 3.15 with Figure 3.5). The resulting forest mask images are shown in Figure 3.15.

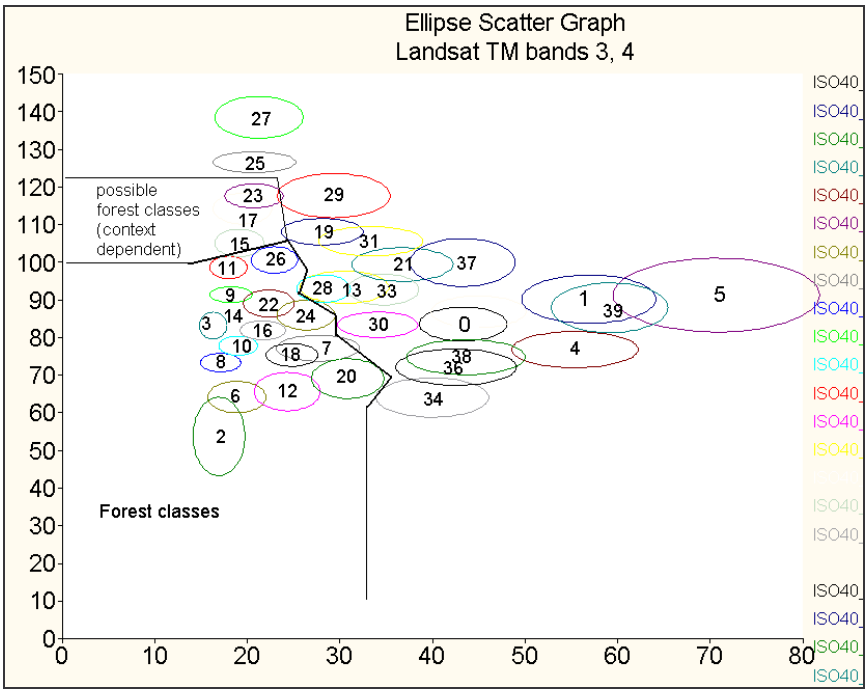

Figure 3.13 Scatter graph for Landsat TM band 3 and 4, with the resulting classes from unsupervised classification (ISOCLASS routine of WinChips).

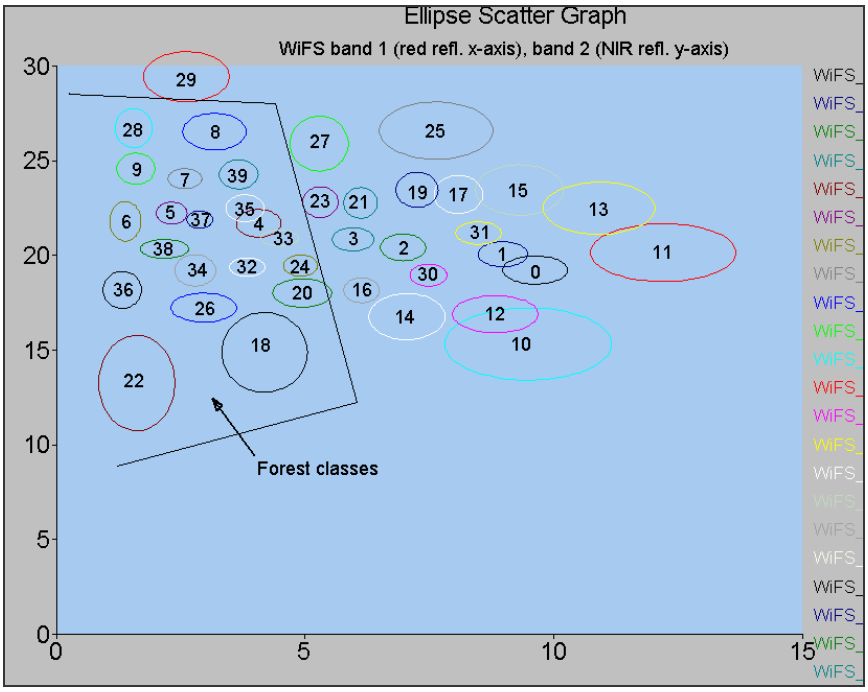

Figure 3.14 Scatter graph for WiFS band 1 and 2, spectral clusters defined by unsupervised classification.

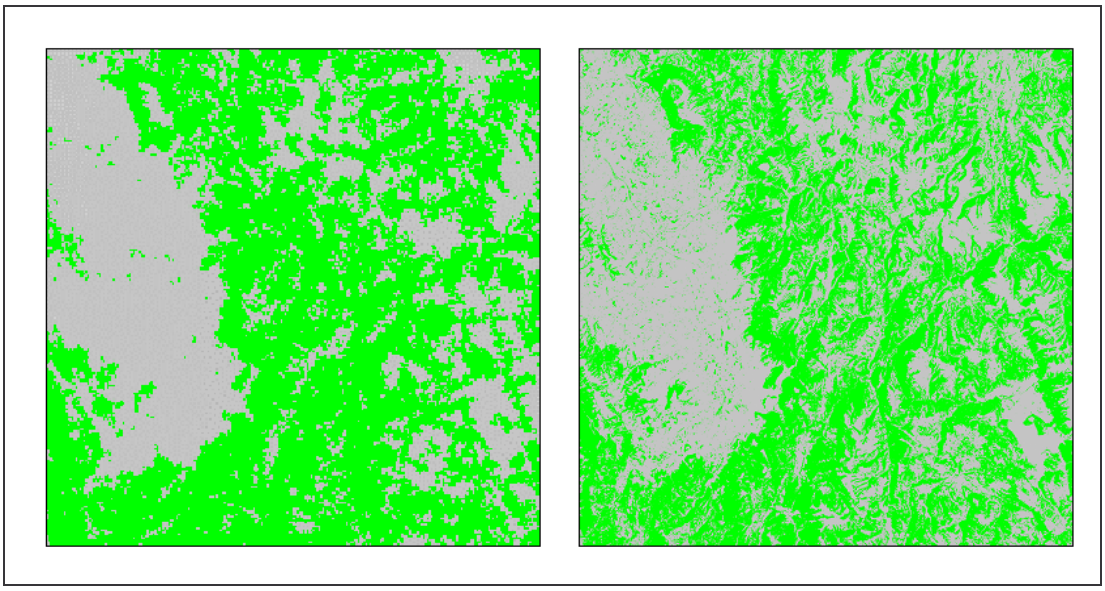

Figure 3.15 Forest -non forest masks from classified images. To the left derived from classification of WiFS image, pixel size 200m, over all forest cover 54.9 %. To the right as derived from classification of Landsat TM image, pixel size 25 m, over all forest cover 44.9%. Extent of image area 50*50 km.

3.3.4 Satellite images, metrics derivation and display

In the next step of image analysis, the two classified images were processed using the modified Fragstats program. As with the synthetic images, the window size was 3*3 km, so

the maximum number of windows for which the indices could be calculated was 256. The results can be displayed in map format, as illustrated in Figure 3.16 below.

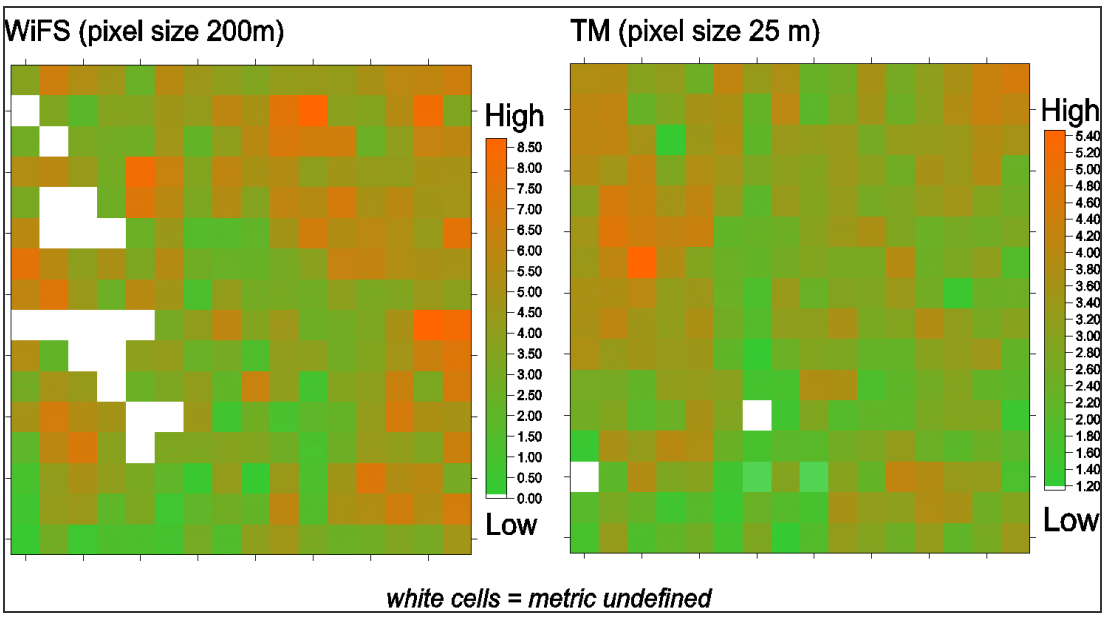

Figure 3.16 Spatial configuration of the values of the Matheron index, calculated from the forest mask images shown in Figure 3.15.

Statistical analysis of the per-window values of the metrics showed that the values from the two different sensors are not as well correlated as the synthesised images at similar resolutions. The plots in Figure 3.17 show the relation between the values derived from TM and WiFS data for the PPU and SqP metrics. Correlations were found between the Matheron Index and the Square-Patch metric; as derived from Landsat TM and IRS - WiFS data respectively (for M: $R^2 = 0.237$, for SqP: $R^2 = 0.393$) – for the PPU metric there was no correlation between the values derived for the different sensors ($R^2 = 0.04$) – which indicates that the landscape property of 'having a certain number of patches per unit area' is level (or sensor) -specific and not scalable or possible to translate between resolutions.

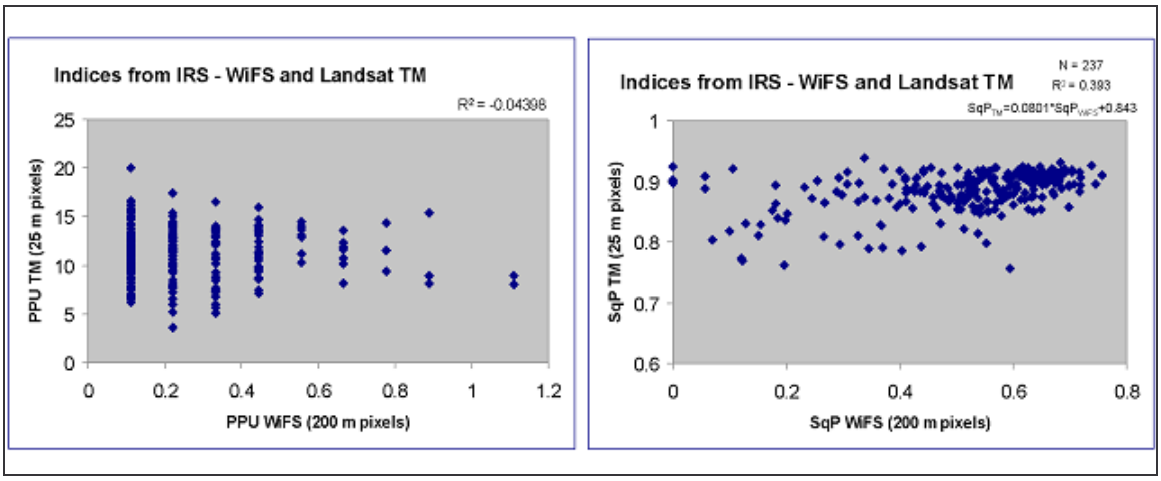

Figure 3.17 Comparison of metrics values between data sources. To the left the PPU values from TM and WiFS respectively are plotted, note that the area unit is km^2, which for WiFS data correspond to only 25 pixels, thus the very low values compared to the TM data. To the right. SqP values, vague trends are found in the relation between the values from the two sensors.

As a 'verification' of the reliability of the overall description of the forest distribution derived from the two images, the forest area in each window was compared, Figure 3.18 shows a plot of this relation. The bias towards a larger area being classified as forest is apparent, but the overall relation is satisfactory, and thus it has been confirmed, that the low correlations between the values of the spatial metrics owe to their response to scaling.

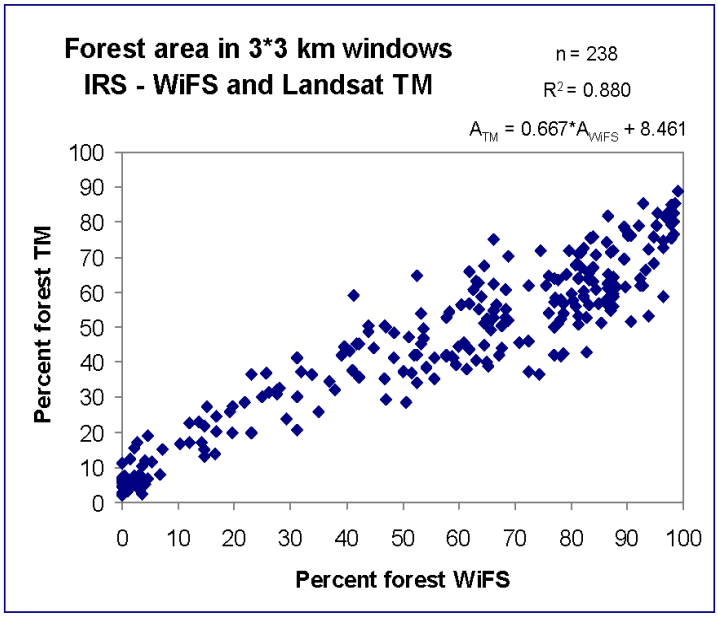

Figure 3.18. Forest cover in windows with forest cover >0. The area estimates appear to be well in accordance.

The Matheron index, as derived from the two image types, did not behave as well as expected from the simulated images, as seen in Figure 3.19, left side. This is assumed to result from a

combination of differences in classification and scaling effects. It can also be attributed to the effect of windows with only a few forest pixels, where their spatial organisation has a large influence on the value of M. This assumption is confirmed by applying a forest cover mask to exclude windows with less that 10 % forest cover in the TM image, which improves the correlation coefficient to 0.467. In order to assess the amount of influence by scaling effects, a forest mask image with pixel size 200 m was generated from the forest mask derived from TM data at a pixel size of 25 m. The comparison of these two images (shown in Figure 3.19, right side) produces a better correlation, although still far from what could be expected from the synthesised images. A possible explanation to this 'under-performance' is that the degradation processes applied in the described procedure (section 3.1) are not optimal. Therefore a degradation process might be required which takes into account the influence of sensor behaviour, such as point spread function and the spectral characteristics of the bands used.

Finally, a 'multi-spectral' approach was tried in order to increase the information content of the maps of spatial metrics. A possible output from a combination of the least correlated metrics (found according to the methods described by Riitters *et al* (1995)) is shown in Figure 3.20. It is possible to distinguish different regions in terms of structural properties, although guidelines for interpretation and possibly classification or regionalisation based on these remain to be developed.

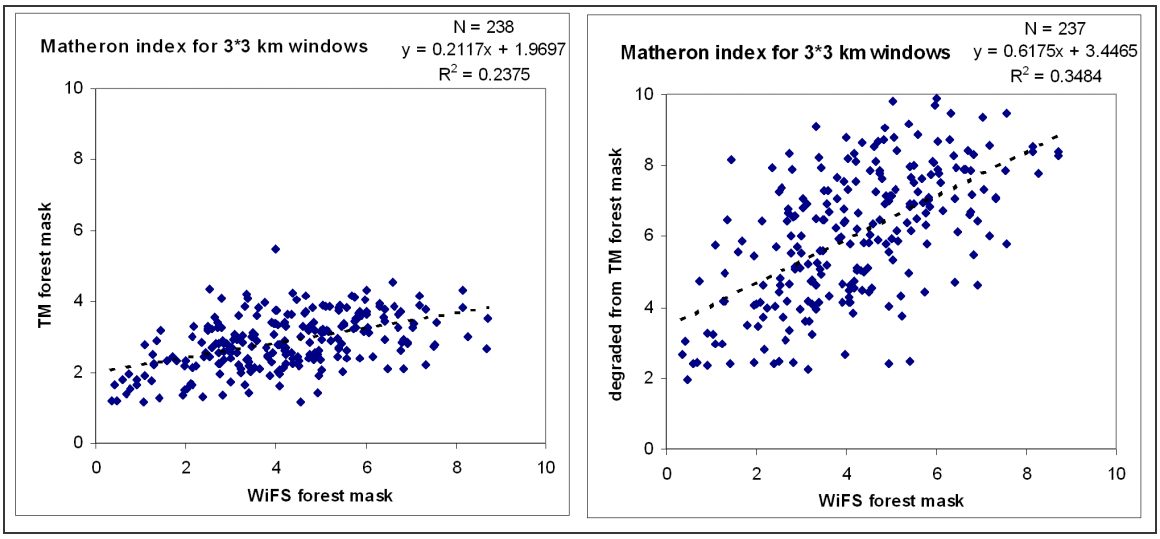

Figure 3.19 To the left M derived from WiFS data with pixel size 200 m plotted against M derived from TM data with pixel size 25 m. To the right M derived from WiFS data with pixel size 200 m plotted against M derived from TM data degraded to pixel size 200 m.

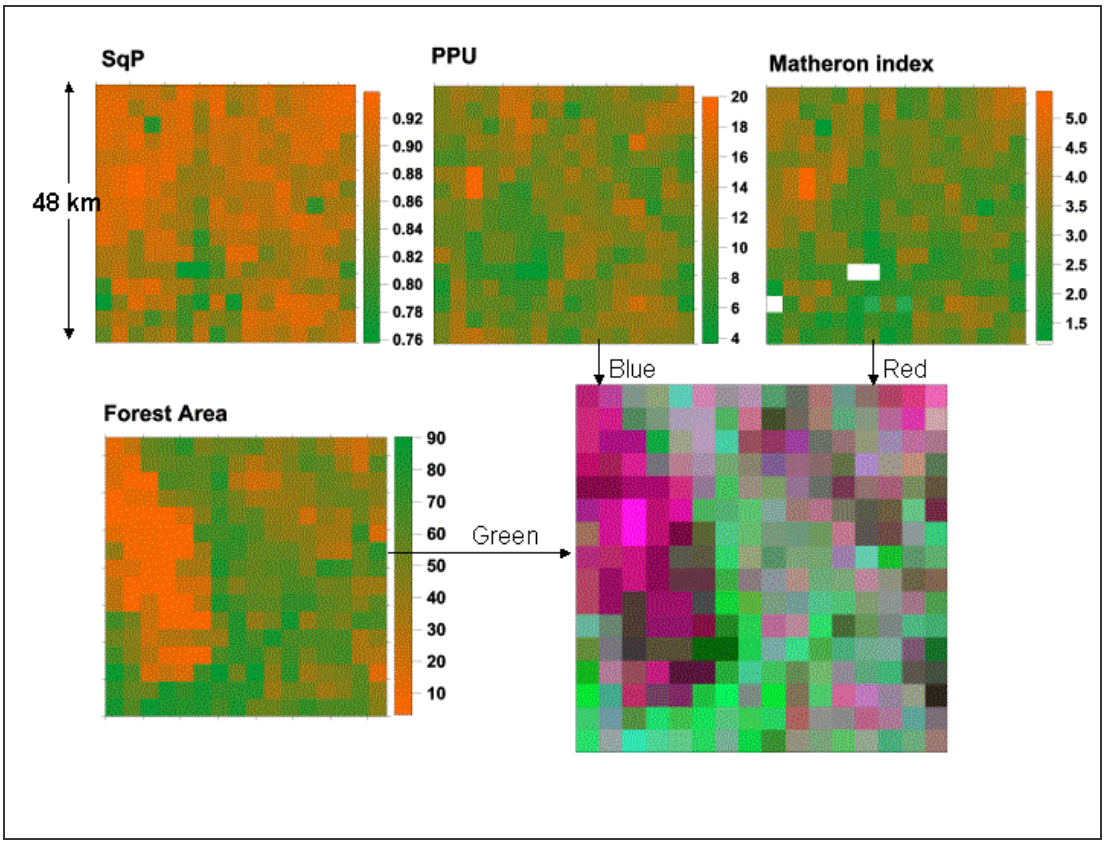

Figure 3.20 Spatial metric maps displayed together as different 'channels' in a false colour image. In this example the indices calculated from the Landsat TM based forest-non-forest map. Cell size 3 km, in a grid of 16*16 cells.

3.4 Discussion and Conclusion

In this study, the Matheron index and the SqP metric are observed to change consistently with the scale of observation, while PPU the metric changes in a more unpredictable way, so as an indicator of fragmentation across scales, this metric must be used with caution. Nevertheless trends are observed for all three metrics following grain size, and it is thus assumed that this procedure of degradation of images, calculation and graphical display of metrics can be improved for use in landscape structure assessment. The results obtained from degradation of simulated images demonstrate that this relationship exists and has a potential for describing landscape structure. The apparent increase in fragmentation as expressed by relative edge length and the apparent decrease in fragmentation as expressed in number of patches are both artefacts of the scaling process. The correlations found between the metrics as derived from TM and WiFS images respectively are lower than the correlations found between the same grain sizes in synthetic images, but the order is the same: SqP values are more consistent than M values, which are again more consistent than the PPU values.

The differences in the values of the metrics investigated here underline the difficulties in quantifying the concept of fragmentation, and confirm the assumption that landscape structure will manifest itself in different ways at different scales of observation. Furthermore, the forest distribution in the test area appears to be related to the topography of the landscape, thus separate experiments should be performed in structurally different areas, in order to assess the influence of the physical setting of the landscape.

Remote sensing provides synoptic images at different scales, potentially making it a powerful tool for applications in multi-scale landscape analysis, including use as illustrations and maps that highlight areas with a particular landscape structure, such as very fragmented or very diverse patterns. Still, the users will have to deal with data from different sensors, often recorded at different times, under different conditions, so it is not trivial to derive comparable land cover maps - something crucial to the comparison of spatial indices.

Assuming that the metrics investigated in this chapter are related to fragmentation processes or the connectivity of the landscape elements (Mertens and Lambin 1997, Hargis *et al* 1998), the analyses carried out here show that it is possible to use processed EO-data to assess structural parameters of importance to forest ecology, and to compare them at different scales and over time, supplying a structural dimension to forest monitoring and change detection.

The methods demonstrated here has potential for operational use, however before the moving windows approach is applied to larger datasets, further assessment of sensitivity to data structure and scaling effects must be carried out. Also more sophisticated though computationally demanding metrics should be tested. Such work could include development of weighted edge metrics, as well as a modified Matheron index to be used on images with more that two land cover classes (Mead *et al* 1981, McGarigal and McComb 1995, Petit and Burel 1997). The pre-processing (first of all classification) of EO data before metrics are calculated could be improved by application of edge preserving smoothing, segmentation and/or neural networks (Wilkinson 1996). For the interpretation of metrics values and their relation to ecological processes, multiple regression of metrics such as the ones studied here or other parameters describing ecological (and physical landscape) conditions should be carried out. This will aid the understanding of what the indices depend on identification of inter-relations and redundancies (Riitters *et al* 1995). The inclusion of indices derived from classifications of aerial photos of the area (preferably at or below one meter resolution) could aid in relating ground observations of forest structure to metrics derived from high- and medium resolution satellite data (Pitt el al 1997, Petit and Burel 1997, Wulder 1998).

In the studies related to this thesis, the results presented here led to focusing of further studies on the comparison of maps derived directly from satellite imagery with CORINE land cover data, which are mostly based on vectorised, high-resolution satellite imagery. In the current, limited study, ‘moving windows’ approach with square sub-landscapes was used for

derivation of spatial metrics. Better alternatives may however be available in form of geo-referenced polygons with the borders of watersheds or administrative units (Weber and Hall 2001, Vogt et at 2003) – to which the spatial properties as expressed in the various metrics can be assigned. This seemed a promising way of addressing the MAUP, and thus a combination of these two approaches was tested in subsequent studies, described in the following chapter.
